JOURNAL OF MORPHOLOGY 269:1181–1196 (2008)

Three-Dimensional Reconstruction of the Stomatostylet and Anterior Epidermis in the Nematode *Aphelenchus avenae* (Nematoda: Aphelenchidae) With Implications for the Evolution of Plant Parasitism

Erik J. Ragsdale,[1]* John Crum,[2] Mark H. Ellisman,[2] and James G. Baldwin[1]

[1]*Department of Nematology, University of California, Riverside, California 92521*
[2]*National Center for Microscopy and Imaging Research, University of California, San Diego, California 92063*

ABSTRACT A three-dimensional model of the stomatostylet and associated structures has been reconstructed from serial thin sections of *Aphelenchus avenae*, a representative of Tylenchomorpha, a group including most plant parasitic nematodes. The reconstruction is compared with previous work on bacteriovorous cephalobids and rhabditids to better understand the evolution of the stylet and its associated cells. Two arcade syncytia ("guide ring") line the stylet shaft, supporting the hypothesis that the stylet shaft and cone (into which the shaft extends and which is not lined by syncytia) are homologous with the gymnostom of cephalobids, the sister taxon of tylenchids. Epidermal syncytia, HypA, HypB, HypC, and HypE, line the cephalic framework, vestibule, and vestibule extension, congruent with the hypothesis that these components are homologous with the cephalobid cheilostom. Relative to outgroups, HypC is expanded in *A. avenae*, enclosing sensilla that fill most of the cephalic framework. The homolog of syncytium HypD in the cephalobid *Acrobeles complexus* is not observed in *A. avenae*. Arcade syncytia are reduced compared with those of cephalobids. Stylet protractor muscles in *A. avenae* are homologous with the most anterior set of radial muscles of cephalobids. Observations to date test and verify our previous hypotheses of homology of the stomatostylet with respect to the stoma of bacteriovorous outgroups. Reconstruction of the stegostom and pharynx will provide further tests of homology and evolution of feeding structure adaptations for plant parasitism. J. Morphol. 269: 1181–1196, 2008. © 2008 Wiley-Liss, Inc.

KEY WORDS: *Acrobeles complexus*; arcade syncytia; *Caenorhabditis elegans*; Cephalobomorpha; feeding; fine structure; free living; homology; modeling; muscle; phylogeny; stoma; syncytium; transmission electron microscopy

Molecular phylogenies often raise questions of morphological evolution where they impose a new paradigm on classical scenarios reliant on opposing ideas of phylogeny. One pressing case of incongruence has been shown in nematodes regarding the evolution of the Tylenchomorpha, which include most species of plant parasitic nematodes, as well as many insect parasites and fungivores. With finer phylogenetic resolution based on molecular analyses, it is apparent that evolution of feeding structures for a parasitic lifestyle can no longer be explained by traditional scenarios, with which new hypotheses of relationships are incongruent. Accumulating evidence suggests that Tylenchomorpha, with a specialized stomatostylet, are sister taxon to or nested within the Cephalobomorpha (Aleshin et al., 1998; Blaxter et al., 1998; Holterman et al., 2006; Meldal et al., 2007; Nadler et al., 2006; Smythe and Nadler, 2006), which lack a stylet and instead have an open stoma characteristic of microbivores. Our understanding of morphological evolution necessarily begins with addressing homology questions. Statements of homology are confounded in these nematodes by the seemingly huge morphological leap from the relatively simple open stoma of microbivores to the complex hypodermic needle-like feeding apparatus of plant parasites. Classical hypotheses of the evolution of the stomatostylet in Tylenchomorpha considered the entire stoma of free-living nematodes to be homologous with the entire stylet in various formulations, usually following a transformation series including several other taxa as intermediates between cephalobids and tylenchids (Thorne, 1961; Andrássy, 1962, 1976; Goodey, 1963; De Grisse, 1972). These character transformations have now been challenged by revised hypotheses in light of new phy-

Additional Supporting Information may be found in the online version of this article.

Contract grant sponsor: United States National Science Foundation; Contract grant numbers: DEB 0228692, DEB 0731516; Contract grant sponsor: Department of Agriculture; Contract grant number: USDA 00903; Contract grant sponsor: National Institutes of Health (NIH); Contract grant number: P41 RR04050.

*Correspondence to: Erik J. Ragsdale, Department of Nematology, University of California, Riverside, CA 92521.
E-mail: erik.ragsdale@email.ucr.edu

Published online 20 June 2008 in
Wiley InterScience (www.interscience.wiley.com)
DOI: 10.1002/jmor.10651

© 2008 WILEY-LISS, INC.

logenies, based on limited available fine structural data of the stomatostylet (Baldwin et al., 2004a).

New hypotheses of relationships preclude an obvious morphological intermediate between stylet bearing tylenchids and most closely related open stoma bearing nematodes. The potential for difficulties in interpreting feeding structure homologies in these groups demands the choice of an appropriate model taxon for stylet reconstruction. Many Tylenchomorpha are assumed to be poor representatives for understanding stylet origins, because their highly specialized feeding adaptations further confound the morphological disparity between them and outgroups. Recent molecular evidence suggests that the family Aphelenchidae[1], including *Aphelenchus avenae*, assumes a sister taxon relationship to all other non-aphelenchid Tylenchomorpha (Blaxter et al., 1998; Holterman et al., 2006; Meldal et al., 2007). *Aphelenchus avenae* thus occupies a phylogenetic position well suited to its use as a model system for comparison to free-living outgroups and it has been selected as a model herein.

Homologies are supported by their adherence to three criteria: congruence with phylogeny based on independent characters; conjunction, or the nonexistence of putative homologs together in the same taxon; and similarity (Patterson, 1982). Categories of similarity include topological, compositional, functional, developmental, and genetic (Panchen, 1994), which can serve individually as recognition criteria and tests. Hypotheses of homology for cuticular feeding structures, which in many respects are divergent between tylenchids and their closest free-living outgroups, are tested by their relationships to complex underlying tissues. These tissues are presumably the secretory source of the extracellular stylet and associated cuticle (Wright and Thomson, 1981; Endo, 1985). Identities of tissues, including syncytia and muscles, are confirmed by several lines of evidence. Their topological relationships to each other provide initial homology proposals, which can then be scrutinized based on other aspects of similarity and ultimately according to their congruence with independent phylogeny. The anterior epidermal syncytia comprise a stack of successive toroids (rings) that line the cuticle of the feeding apparatus, lips, and body wall. The identities and positions of at least some stoma elements, such as the arcade syncytia and stomatal muscles, are known to be highly conserved from reconstructions of representatives of rhabditids (Albertson and Thomson, 1975; Wright and Thomson, 1981), diplogastrids (Baldwin et al., 1997a), and cephalobids (Van de Velde et al., 1994; Baldwin and Eddleman, 1995; De Ley et al., 1995; Bumbarger et al., 2006). The arrangement of most epidermal syncytia is also conserved between representative cephalobids and rhabditids (Bumbarger et al., 2006). The numbers, positions, and interrelationships of syncytial somal extensions, which extend relatively far posteriad to include the nuclei of the syncytia, are highly conserved and confirm hypotheses of tissue identities. The relationships of epidermal syncytia to sensory structures, such as is inferred by relative locations of sensillum socket cells, are in many respects conserved and thus offer additional support to homology statements.

Studies employing TEM have afforded a much clearer understanding of homologies at a more fundamental (i.e., cellular) level, as some structures are only barely or not at all visible by light microscopy. Yet even serial thin sectioning has been limited in its resolution of complex cells, with minute processes and contacts being difficult to recognize as associated with a particular cell body. Baldwin et al. (2004a) recognized a body of fine structural research of the tylenchid stylet that predates our understanding of stoma homologies in Chromadorea, but which has nevertheless stimulated questions for more sophisticated examination. In this work, morphology is analyzed using three-dimensional (3D) reconstruction of more complete serial thin sections, with the aid of digital imaging and recently developed computer software for alignment and model building and rendering. These tools have made visualization of elusive but significant features more tractable. By establishing homologies of tissues in the level of detail afforded by 3D reconstruction, this work builds upon comparably detailed reconstruction in a free-living outgroup, *Acrobeles complexus* (Cephalobomorpha) (Bumbarger et al., 2006), as part of a larger scale laboratory effort. With respect to what is also known of corresponding tissues in the model nematode *Caenorhabditis elegans* (Rhabditomorpha), a more distant outgroup, we test homologies of the stylet and associated cuticular structures with specific components of the cephalobid stoma.

The regions making up the stoma of cephalobids and rhabditids are the units of analysis for stomatostylet homologies herein. Stoma regions were originally defined by their apparent division, in light microscopy observations, into a series of distinct sets of cuticular thickenings or rhabdia (Steiner, 1933); however, the terminology was later expanded based on fine structure to reflect a clearer understanding of stoma components, including homologies across several microbivorous taxa (De Ley et al., 1995). Thus, three basic divisions are identified as the units of a comparative study between cephalobids and tylenchids (see Fig.

[1]Herein the authors adhere to the classification of De Ley and Blaxter (2002, 2004) for infraordinal and higher level taxa, while acknowledging doubts of monophyly of some groups as currently defined. Because classification within Tylenchomorpha does not yet reflect recent developments in phylogeny, formal names below infraorder follow the systems of Hunt (1993) and Siddiqi (2002).

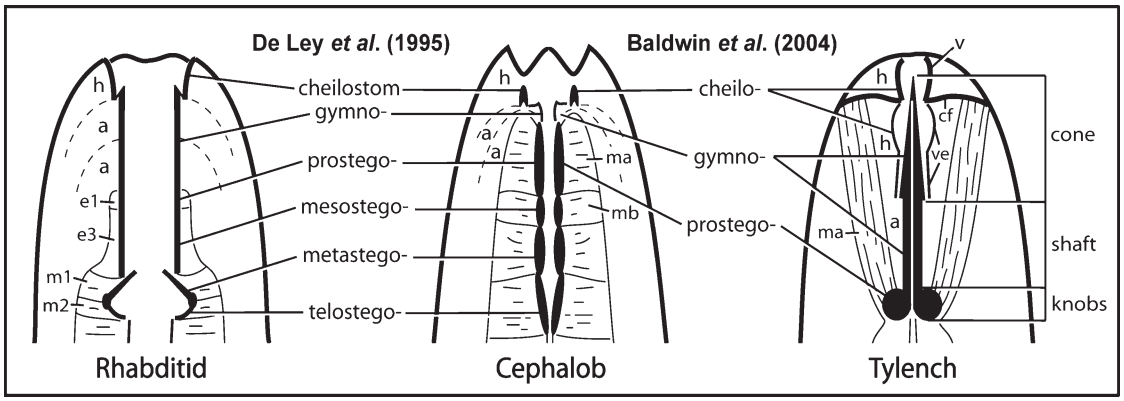

Fig. 1. Diagrammatic representation of stoma components of rhabditids and cephalobids, with hypotheses of homologies extended to tylenchids. Generalized rhabditid is redrawn from De Ley et al. (1995); cephalobid and tylenchid are redrawn from Baldwin et al. (2004a). a, arcade syncytia; cf, cephalic framework; e1 and e3, stomatal epithelia; h, epidermal syncytia; m1, m2, ma, and mb, stomatal muscle cells; v, vestibule; ve, vestibule extension.

1): i) the cheilostom, which is the cuticle continuous with the body wall and secreted by underlying epidermis; ii) the gymnostom, which is an area of thickened cuticle surrounded by two syncytial arcade rings; iii) the stegostom, which is the part of the stoma surrounded by the anterior end of the pharynx, including muscle and epithelia, and characterized by a triradiate lumen, although homologies implied for stegostom components at a finer level (e.g., pro-, meso-, meta-, and telo-stegostom) between cephalobids and rhabditids have since been challenged (Dolinski et al., 1998). The goal of this study is to test whether the cheilostom, gymnostom, and stegostom are represented by readily identifiable homologs in the tylenchid stomatostylet.

MATERIALS AND METHODS

Aphelenchus avenae Bastian (strain RGD103) was obtained courtesy of Dr. Robin Giblin-Davis and maintained on *Monilinia fructicola* in LG potato dextrose agar medium. Nematodes were frozen in a Bal-Tec HPM 010 high-pressure freezer and then dehydrated, fixed, and stained en bloc via freeze substitution using a Reichert-Jung CS Auto freeze substitution apparatus in an acetone cocktail of 3% osmium tetroxide and 1% uranyl acetate. Nematodes were processed in custom stainless-steel chambers to prevent specimen loss, as described by Bumbarger et al. (2006). During freeze substitution, nematodes were held at −90°C for 40 h, warmed at a gradual rise of 4°C/h to −60°C, held for 30 h, and then warmed again at 4°C/h to −20°C. Following freeze substitution, specimens were rinsed several times over 4 h in acetone at −20°C. Specimens were serially infiltrated with 25, 50, and 75% Epon 812 resin over the course of 24 h, followed by three changes to 100% resin without accelerator over another 24 h and a final change to 100% resin with accelerator for 3 h in molds shaped as 25 × 75 mm^2 microscope slides. Resin was polymerized at 60°C for 24 h.

Specimens, embedded in Epon 812 slides, were screened by differential interference contrast (DIC) microscopy using a Nikon E600 DIC-LM to identify adult females without tissue damage. Through-focus video vouchers were obtained with a Spot RT color 2.2.1 camera and the software Openlab 3.1.7 on a Macintosh G4 computer; vouchers were later used to produce measurements for calibrating dimensions of the reconstructed model. Specimens were then re-embedded in blocks for sectioning. Serial silver-gold sections (70 nm thick) of specimens were taken on a Sorvall MT6000 microtome with a Microstar diamond knife. Sections were mounted on pioloform films on Synaptek wide-slot, nickel grids. Mounted sections were post stained with methanolic uranyl acetate and lead citrate.

Sections were imaged using a Philips Tecnai T12 transmission electron microscope operating at 120 kV. Images of sections were acquired in the form of montages of 4, 9, or 16 individual images each taken with a Gatan US1000 2k × 2k pixel camera and automatically assembled with Digital Micrograph. Imaging was conducted at the Center for Advanced Microscopy and Microanalysis (CFAMM) at the University of California, Riverside. Ordered images of serial sections were prepared for stack assembly by reducing depth to 16 bit, reducing pixel density to facilitate manageable file sizes, and standardizing canvas size using scripts written for ImageJ (http://rsb.info.nih.gov/ij/) and Adobe Photoshop 7.0 (San Jose, CA). Images were converted from TIFF to the MRC stack format, stacked images were manually aligned, individual cell contours manually traced, and contour-based mesh models of cells constructed using the software package IMOD (Kremer et al., 1996). Models were transferred to Blender 2.42 (blender3d.org), an open source ray tracing and mesh modeling package, for final visualization and production of model figures and animations. All model components except stylet knobs were reconstructed from a single specimen alignment; stylet knobs were reconstructed from a separate specimen but then were united with the rest of the stylet from the main model to form a composite model object. Four specimens were sampled to check for intraspecific variation, including one specimen fixed by wet fixation (rather than freeze substitution) in 2.5% glutaraldehyde and 2% osmium tetroxide but with preparations otherwise consistent with other specimens.

Terminology specific to syncytial morphology follows Wright and Thomson (1981) and Bumbarger et al. (2006).

RESULTS

Three-dimensional reconstruction identified complex cells closely associated with the stylet. Regardless of complexity, phylogenetically conserved cells and associated regions of cheilostom, gymnostom, and stegostom could be readily identified by general aspects of similarity with outgroups. Cell names, consistent with those originally applied in *A. complexus*, are based on puta-

TABLE 1. Abbreviations used for names of stomatal tissues

Abbreviation	Annotation	No. of cells	Applicable taxa
HypE	Anterior (nose) epidermal syncytium E	1	*Acrobeles complexus, Aphelenchus avenae*
HypD	Anterior (nose) epidermal syncytium D	1	*A. complexus*
HypC	Anterior (nose) epidermal syncytium C	1	*A. complexus, A. avenae*
HypB	Anterior (nose) epidermal syncytium B	1	*A. complexus, A. avenae*
HypA	Anterior (nose) epidermal syncytium A	1	*A. complexus, A. avenae*
Hyp4	Anterior (nose) epidermal syncytium 4	1	*Caenorhabditis elegans*
Hyp3	Anterior (nose) epidermal syncytium 3	1	*C. elegans*
Hyp2	Anterior (nose) epidermal syncytium 2	1	*C. elegans*
Hyp1	Anterior (nose) epidermal syncytium 1	1	*C. elegans*
e1	Anterior stomatal epithelial cell	1	*C. elegans*, other rhabditids, diplogasterids
e2	Marginal cell	3	All taxa
e3	Posterior stomatal epithelial cell	1	*C. elegans,* other rhabditids, diplogasterids
ma	Most anterior stomatal muscle	3	*A. complexus*, other cephalobids
mb	Second most anterior stomatal muscle	3	*A. complexus*, other cephalobids
m1	Most anterior stomatal muscle	3	*C. elegans*, other rhabditids, diplogasterids
m2	Second most anterior stomatal muscle	3	*C. elegans*, other rhabditids, diplogasterids

tive homology with cells in the latter nematode following initial homology proposals.

Cheilostom

The cells associated with the cheilostom comprise the putative HypE, HypC, HypB, and HypA syncytia (see Table 1 for annotations of abbreviations). These syncytia fill most of the cephalic framework, a hexaradiate structure separating anterior tissues into compartments by cuticular walls (Figs. 2B and 4A), and are also associated with that part of the guiding apparatus posterior to the framework (Fig. 2C).

Putative HypE is the outermost anterior epidermal syncytium (Fig. 2B,D), and lies just anterior to the main mid body epidermal syncytium along the body wall. It lines the body wall cuticle up to the posterior boundary of the framework. At its anterior end, HypE includes six thin, concave pockets (Fig. 2E) consisting mostly of tonofilaments (Fig. 4B), through which the stylet protractor muscles (stegostom) attach to the six vertical (longitudinal) blades of the framework. Where the muscles attach, the blades of the framework spread horizontally (transversely) into concave pockets. Anterior body wall muscles also insert into these pockets as well as into the rest of the circumference of the toroid of HypE. HypE sends six short, anterior projections, which are each associated with a bundle of sensory cells, into the toroid of HypC, one in each of the sextiles of the framework (Fig. 4B). The sheet-like distal periphery of the toroid has four medial ridges or cords (one dorsal, one ventral, two lateral; Fig. 2E). The more prominent of these cords are the dorsal and ventral (although the dorsal cord is compressed by the dorsal stylet protractor along part of its length), which are contiguous with the medial apices of the toroid's anterior pockets. At these pockets, the dorsal and ventral cords are perforated, forming a loop, through which protractor muscle branches come together from either side of each cord and insert into the pockets (Fig. 2E). Posterior to the toroid, the dorsal and ventral cords are somal extensions. The lateral cords extend into long, attenuated, and apparently pseudosomal extensions, although these were not traced definitively to their ends. All of these extensions become separated from the body wall by the posteriorly adjoining body wall epidermis, with which they maintain an association. Posteriorly the ventral somal extension wraps around the ventral bundle of somal extensions of the arcade syncytia (gymnostom), and putative HypA and HypB (Fig. 2D). The dorsal cord is also associated with dorsal somal extension of the posterior arcade syncytium along much of its length, and this contact remains continuous along the somal extension. The dorsal somal extension forms a bundle with the two somal extensions of HypC (Fig. 2D). The lateral somal extensions of HypE each send a process to contact the ventrolateral extensions of the posterior arcade syncytium (Fig. 2D).

Near the base of the framework, a relatively large volume between the toroid of HypE and that of the adjacent epidermal syncytium, putative HypC, is occupied by cells of the nematode's anterior sensilla. Positioned between the HypE and HypC toroids are the socket cells of the amphids, cephalic sensilla, and outer labial sensilla. Between these two toroids the sensillum dendrites enter the cuticle of the framework, which is contiguous with the cuticular lining of the dendrites.

Putative HypC is the most anterior epidermal syncytium of the nematode. Together with the anterior extensions of HypE, labial and cephalic sensilla, and other dendrites terminating within itself, HypC fills the entire cephalic framework (Fig. 2A). Thus, HypC is split into sextiles within the frame-

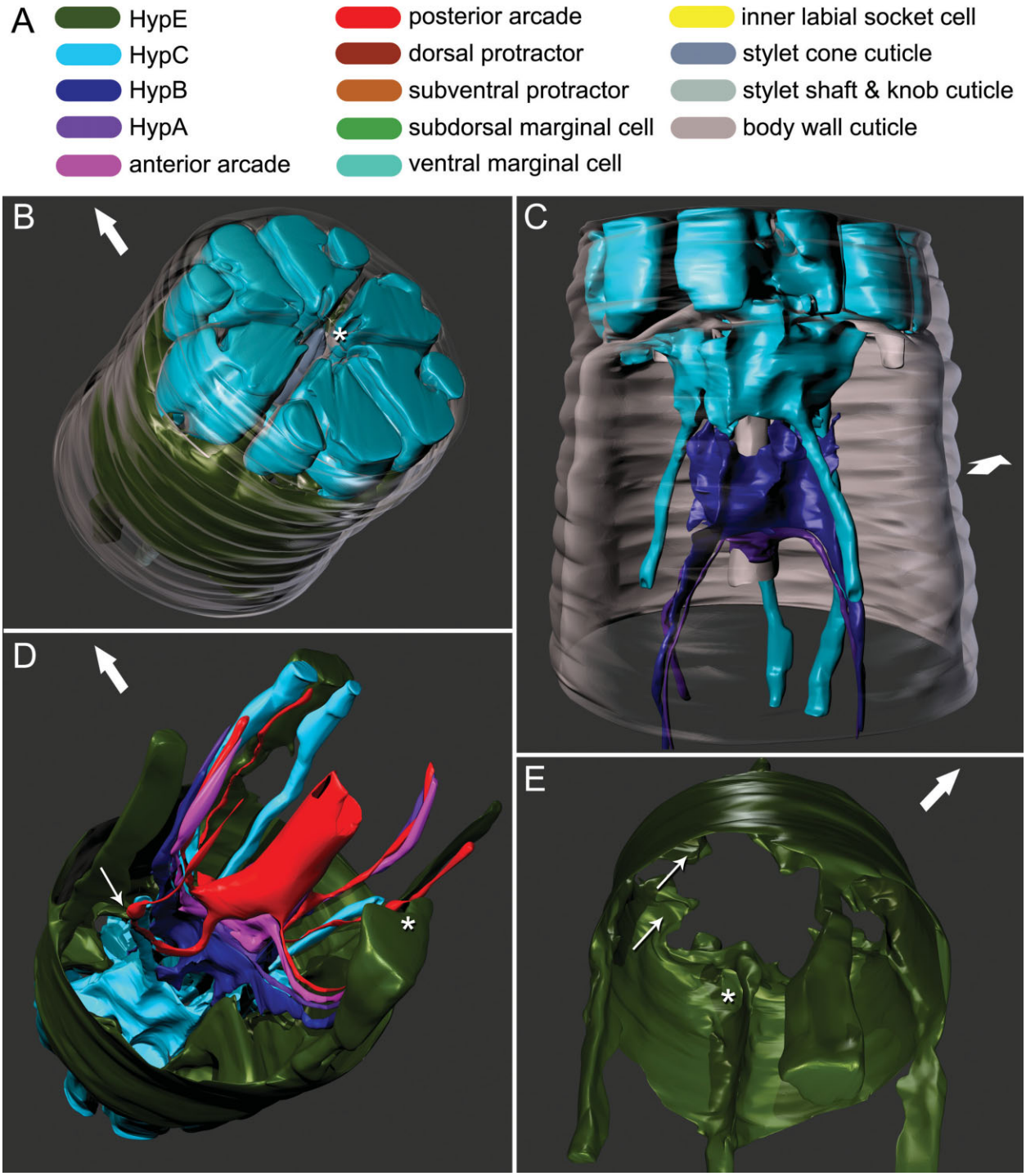

Fig. 2. Three-dimensional reconstructions based on serial TEM sections of tissues and cuticle of the stomatostylet apparatus of *Aphelenchus avenae*. Body wall cuticle and all somal extensions are truncated posteriorly; body wall cuticle and most anterior epidermis (i.e., HypC) are truncated anteriorly through the tips of the lips. Large arrows indicate dorsal. **A:** Key to cells (applies also to Fig. 3). **B:** Oblique anterior view of HypE toroid, HypC toroid, and the tip of the stylet, all seen through the body wall cuticle (rendered transparent). Asterisk indicates stomatal opening. **C:** Ventral view of HypC, HypB, and HypA toroids lining the cephalic framework (rendered transparent) and the vestibule extension. **D:** Oblique posterior view of all anterior syncytia, including extensions in pseudocoelomic cords. Thin arrow indicates point of contact between lateral somal extension of HypE and ventrolateral somal extension of the posterior arcade syncytium; asterisk indicates incipient groove in somal extension of HypE that envelops ventral pseudocoelomic cord posteriorly. **E:** Oblique posterior view of HypE toroid, showing some cords and other medial structures. Thin arrows indicate examples of pockets for attachment of somatic and stylet protractor muscles; asterisk indicates ventral loop through which protractors meet.

work (Fig. 4A), the subdorsal and subventral of these being further cleft anteriorly by the cuticle of the cephalic sensilla. Medially the syncytium lines the vestibule and vestibule extension as well as the cuticle of the inner labial sensilla, which is itself contiguous with the vestibule (Fig. 4A,B). Posterior to the framework, HypC is attenuated and does not enclose the various sensilla and internal receptors as it does within the framework. At the base of and posterior to the framework, HypC forms several connections with HypE, the prominent dorsal and ventral ones being maintained about as far posteriad as HypC lines the vestibule extension. At the posterior end of its toroid, HypC forms six connections with each of the anterior projections of its other neighboring epidermal syncytium, putative HypB (Figs. 2C,D, 3C, and 4D). On the dorsal side, the HypC syncytium extends posteriad and splits into two robust subdorsal somal extensions (Fig. 3A). The somal extensions of HypC run adjacent to the dorsal branch of the dorsal protractor muscle, ultimately establishing contact with the dorsal somal extension of HypE (Fig. 2D). At the level of the split of the two dorsal somal extensions of HypC, and just posterior to its contact with HypE, HypC contacts the dorsal somal extension of the posterior arcade syncytium. Additionally, at the level of this split, a minute dorsal process wraps around a process of HypB that projects anterior from the main dorsal branch of HypB, and posterior to the other dorsal connection (Fig. 4D). HypC also has two lateral, posterior pseudosomal extensions (Fig. 3A) that, in contrast to somal extensions, definitely lack nuclei; each surrounds the ciliary region of an internal receptor dendrite and terminates at about the level of the gymnostom. The pseudosomal extensions each make contact with a dorsolateral somal extension of the posterior arcade syncytium at and anterior to the point of entry of the internal receptor dendrites into the former (Fig. 5B).

The toroid of the putative HypB syncytium is just posterior to that of HypC, and is much smaller. Most of the toroid is concentrated in six distally projecting blades (one dorsal, one ventral, two dorsolateral, two ventrolateral) that extend into anterior processes (Fig. 3B), each of which make a connection (the dorsal makes two) with HypC. Between these points of connection are the inner labial socket cells, through which dendrites enter and adjoin the cuticle of the vestibule extension (Fig. 3C). Posteriorly the HypB toroid is separated from the vestibule extension and is replaced by that of the putative HypA syncytium. HypB has one ventral and one lateral (left) somal extension. The right, lateral posterior projection of the syncytium abruptly terminates closely posterior to the toroid (Fig. 3B).

Putative HypA is the most posterior syncytium lining the vestibule extension (Fig. 2C), except for the anterior margin of the anterior arcade syncytium (gymnostom), which adjoins HypA at the tip of the vestibule extension. HypA is the smallest syncytium of the cheilostom and has a relatively simple morphology. At its widest the toroid has three rounded apices, which are ventral and left and right dorsolateral (Figs. 3D and 4E), each extending posteriad into a somal extension. The lateral and ventral somal extensions of HypA, as well as those of HypB, HypC, and gymnostom syncytia, are separated from the buccal cuticle by the stylet protractor muscles. The somal extensions are grouped in bundles ("pseudocoelomic cords") that are nestled in the narrow gaps between branches of the protractor muscles.

Gymnostom

The cells associated with the gymnostom comprise two arcade syncytia. These syncytia line the stylet shaft, the wall of which extends anteriorly into the wall of the stylet cone (Fig. 3G). Together these two cuticular structures form a tube, the lumen of which acts as a conduit for feeding. The stylet cone is composed of cuticle that is more electron dense, given our preparation methods, than most other types of cuticle found in the stomatal, cephalic, or body wall areas (Fig. 4C,D). The lumen of the cone is at least half the diameter of the cone itself at its base, and proportionally even larger at the tip (Figs. 4A,C,D and 3G,H). The orifice of the stylet cone is a wide ventral slit of almost half the length of the entire cone (Fig. 3G). The cuticle of the cone is embedded with anteriorly projecting, attenuated cuticle of the stylet shaft, readily distinguished by the difference in electron density of its collagen. The cone is entirely replaced posteriorly by the shaft, which is longer and thicker than the cone, the lumen ranging in diameter from less than half to one third that of the shaft itself. From anterior to posterior the shaft gradually changes from circular to triangular in cross section, with rounded ventral and left and right dorsolateral apices (Fig. 5D). Between the apices are grooves that are replaced posteriorly by the weak stylet knobs of the stegostom (Fig. 3G,H); in the grooves are traces of more electron-dense cuticle, and of this most markedly within the dorsal groove. The dorsal groove is continuous along the entire length of the shaft where it is not embedded in the cone, giving the appearance of a "seam" (Figs. 4F and 5A,B,D).

Lining the stylet shaft anteriorly is the putative anterior arcade syncytium (Fig. 3E,G). This syncytium also lines the thin, dilated posterior tip of the vestibule extension, thus acting as a flexible link between the stylet and the guiding apparatus (Figs. 3E and 5B). A lobe of the syncytium projects anteriorly on the dorsal side, maintaining a connection with HypA. The toroid of the anterior

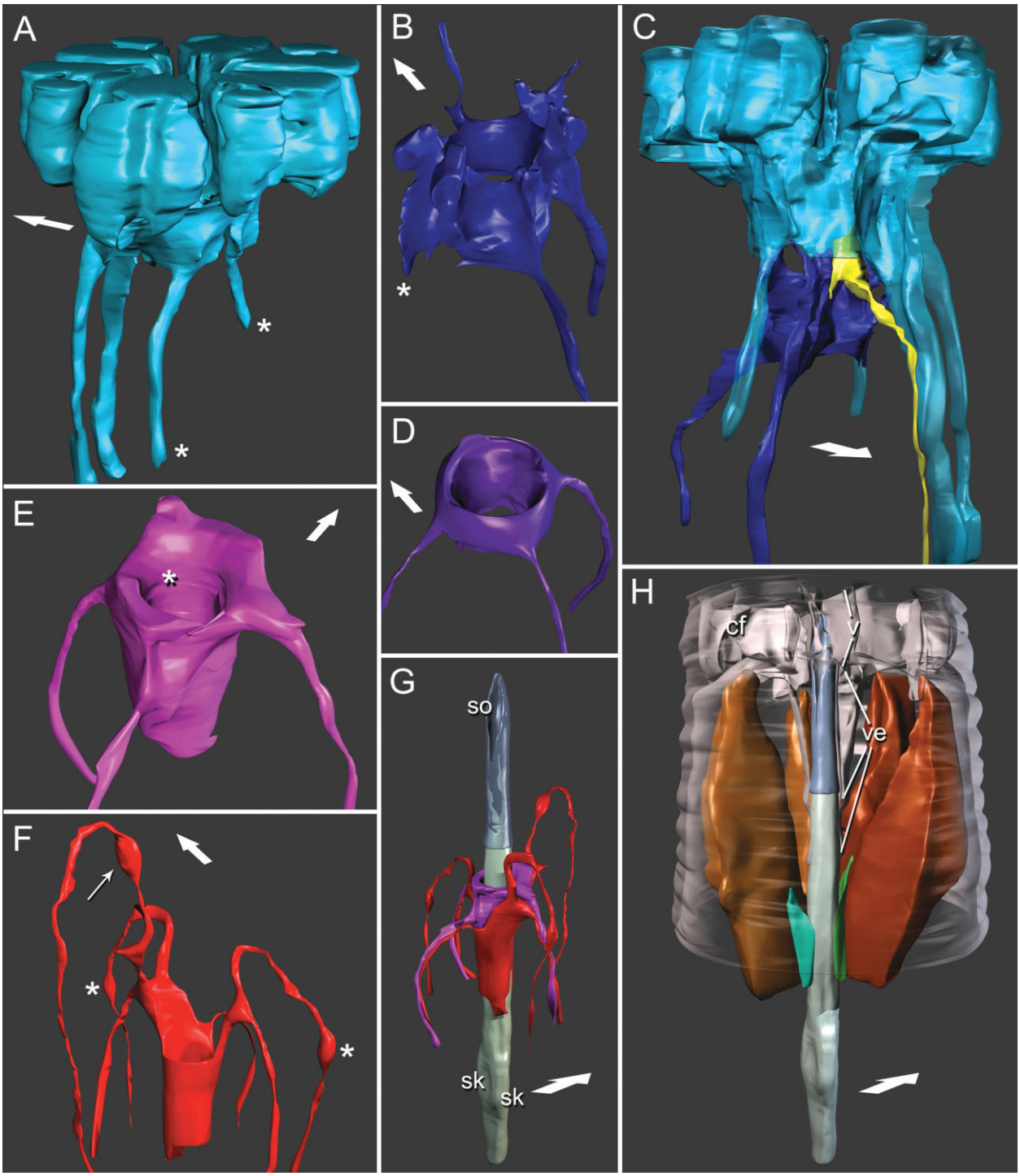

Fig. 3. Three-dimensional reconstructions based on serial TEM sections of tissues and cuticle of the stomatostylet apparatus of *Aphelenchus avenae*. Body wall cuticle and all somal extensions are truncated posteriorly; body wall cuticle and most anterior epidermis (i.e. HypC) are truncated anteriorly through the tips of the lips. Large arrows indicate dorsal. Key to cells (given in Fig. 2). **A:** Lateral view of HypC toroid. Asterisks mark pseudosomal extensions. **B:** Anterior, ventral view of HypB toroid. Asterisk marks asymmetrically "missing" somal extension. **C:** Dorsolateral view of HypC (rendered semitransparent) and HypB toroids, showing the position of a representative inner labial socket cell. **D:** Anterior, ventral view of HypA toroid. **E:** Anterior, ventral view of toroid of anterior arcade syncytium. Asterisk indicates fold accommodating the tip of the vestibule extension. **F:** Ventrolateral view of toroid of posterior arcade syncytium. Thin arrow indicates swelling of somal extension at its contact point with dorsal somal extension of HypE and splitting somal extensions of HypC; asterisks indicate swellings of somal extensions at their contact points with the tips of the pseudosomal extensions of HypC. **G:** Ventrolateral view of stylet lined by arcade syncytia. Stylet cone is rendered transparent; stylet shaft material is shown projecting into thin wall (not lumen) of cone. Reconstruction of stylet shaft and knobs is a composite, the posterior portion (including knobs) reconstructed from a separate dataset of serial TEM sections. sk, stylet knobs (right and left subventral); so, stylet orifice. **H:** Ventrolateral view of the stylet with dorsal and left subventral stylet protractor muscles, as well as ventral and left subdorsal marginal cells. Cephalic framework (cf), to which protractors attach, guiding apparatus (i.e., vestibule, v, and vestibule extension, ve), and peripheral body wall cuticle are rendered transparent. Muscles and marginal cells are cut away anterior to their point of attachment to stegostom; right subdorsal marginal cell is hidden from view behind stylet; right subventral protractor has been removed for clarity.

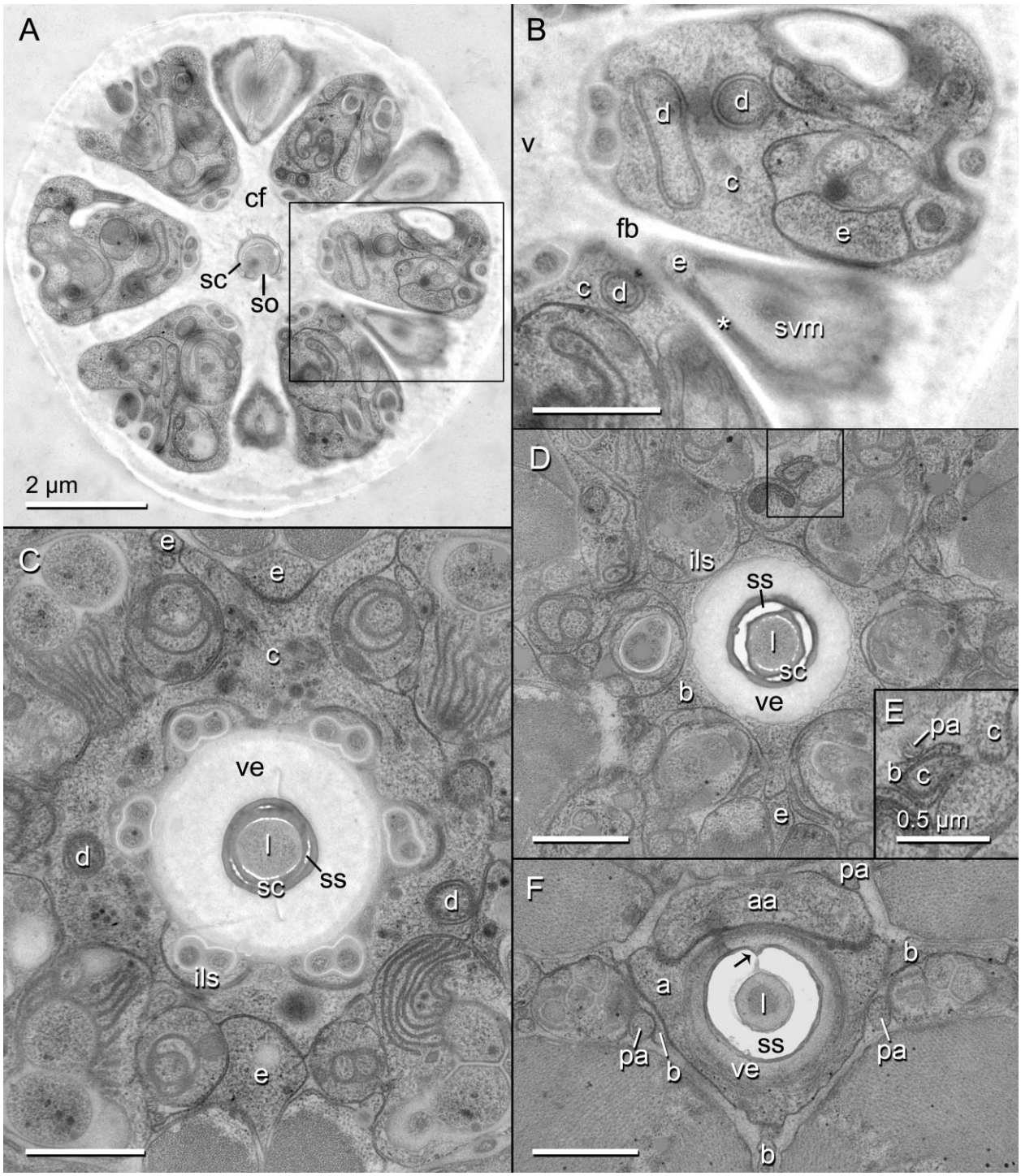

Fig. 4. Transverse TEM sections through the cheilostom of the head region of *Aphelenchus avenae*. Scale bars are 1 µm unless otherwise indicated. **A:** Entire transverse section of nematode showing the cephalic framework (cf), encircling the stylet cone (sc) and dividing sextiles of epidermal and nervous tissue with longitudinal blades. Area within rectangle is enlarged in (B). so, stylet orifice. **B:** Enlarged inset of (A) showing putative HypE (e) and HypC (c) within sextiles of framework, the attachment of the subventral stylet protractor muscle (svm) to a framework blade (fb) through HypE via tonofilaments (asterisk), and the multilamellar dendrite (d) that is expanded in HypC. v, vestibule. **C:** Toroid of HypC lining the vestibule extension (ve) and the inner labial socket cells (ils), and showing several margins of contact with HypE; the anterior extension of stylet shaft (ss, lightly stained) cuticle into the stylet cone (darkly stained) is also shown. l, stylet lumen. **D:** Toroid of putative HypB (b) lining the inner labial socket cells and vestibule extension, here surrounding the stylet cone. Area within rectangle is enlarged in (E). **E:** Enlarged inset of (D) showing connections of processes of HypC and HypB with the dorsal pseudosomal extension of the posterior arcade syncytium (pa). **F:** Toroid of putative HypA (a), lining the posteriorly thinning vestibule extension, and its association with HypB and an anterior lobe of the anterior arcade syncytium (aa); arrow indicates dorsal "seam" of stylet shaft.

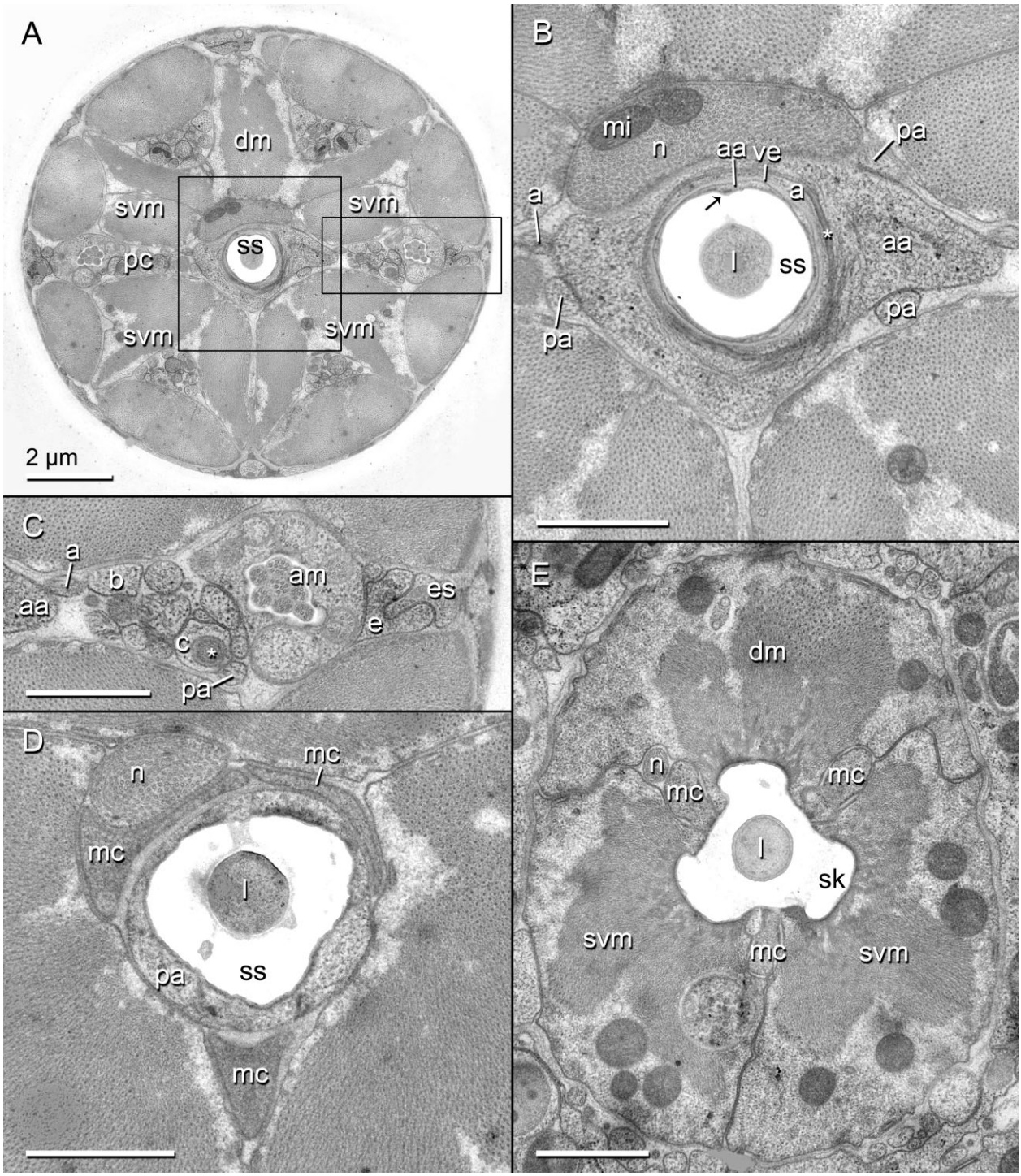

Fig. 5. Transverse TEM sections through the gymnostom and stegostom of the head region of *Aphelenchus avenae*. Scale bars are 1 µm unless otherwise indicated. **A:** Entire transverse section of nematode showing the stylet shaft (ss), surrounding syncytia, and six robust pseudocoelomic cords (pc) separated by six incipient branches of the dorsal (dm) and subventral (svm) stylet protractor muscles. Area within central rectangle is enlarged in (B); area within rectangle to right is enlarged in (C). **B:** Enlarged inset of (A). Toroid of anterior arcade syncytium (aa) lining the stylet shaft and the thinned posterior tip of the vestibule extension (ve); asterisk marks tight junction between the anterior arcade cell and HypA (a); arrow indicates dorsal "seam" of stylet shaft. Also shown is the swollen tip of the pharyngeal neuron (n) associated with the dorsal protractor, including mitochondria (mi). l, stylet lumen; pa, posterior arcade syncytium. **C:** Enlarged inset of (A). A lateral pseudocoelomic cord, showing several syncytial extensions as identified by 3D reconstruction. Asterisk marks one of the multilamellar dendrites just anterior to its entry into the pseudosomal extension of HypC (c). am, amphid; b, HypB; e, HypE; es, mid body epidermal syncytium. **D:** Toroid of posterior arcade syncytium lining the posterior part of the stylet shaft and anterior extensions of the marginal cells (mc). **E:** Triradiate stylet protractor muscles and marginal cells lining the stylet knobs (sk).

arcade syncytium is minor in size relative to most other epidermal syncytia. It has three somal extensions (one ventral, two lateral) that distally exit the stylet region and join the corresponding three pseudocoelomic cords, which are bundles of posterior extensions of several other syncytia as well as some dendrites. The lateral somal extensions each project through the split between the dorsolateral and ventrolateral somal extensions of the posterior arcade syncytium on each lateral side, and are closely associated with the dorsolateral extensions of the posterior arcade syncytium (Fig. 3G).

The putative posterior arcade syncytium is adjacent to the anterior arcade syncytium and lines the posterior portion of the stylet shaft (Figs. 3D,E and 5D). The toroid of the posterior arcade syncytium is also relatively minor. It contacts the anterior projections of the three marginal cells of the stegostom, and has small posterior processes that enter the marginal cells (not shown). In the transition to the stegostom, the posterior arcade toroid persists as three posterior points between the apices of the stylet shaft (not all represented in the model), which are lined by the marginal cells, and are replaced posteriorly by attachment points of the stylet protractor muscles. The posterior arcade syncytium has six somal extensions (one dorsal, two dorsolateral, two ventrolateral, one ventral); each extension projects anteriad for some distance before exiting the central body axis through the splits in the protractor muscles, after which it joins one of the six pseudocoelomic cords (Figs. 2D and 5C). The manner of branching of the lateral somal extensions is symmetrical left and right, the ventrolateral extensions recurving much further anteriorly than the dorsolaterals. The ventrolateral somal extensions are swollen where they contact the pseudosomal extensions of HypC (Fig. 3F). The dorsal somal extension is also swollen where it contacts the dorsal extension of HypE, which is just medial to where it exits through the split of the dorsal protractor muscle (Figs. 3F and 5B). Posterior to this latter connection, the dorsal somal extension contacts the dorsal branch of HypC where the latter splits into its own dorsal somal extensions; just posterior to this connection, it contacts HypB where the latter engulfs the minute process of HypC (Fig. 4E). Posterior to this, it contacts the toroid of HypB; posterior to this contact, it passes and maintains a connection with the anterior arcade syncytium. The ventral somal extension originates just anterior to the point where the toroid attaches to the stylet shaft (Fig. 3G).

Stegostom

The cells associated with the prostegostom comprise three radial, stylet protractor muscle cells (one dorsal, two subventral) interspersed with three epithelial marginal cells (two subdorsal, one ventral) (Figs. 3H and 5E), all of which extend far posteriad into the pharynx (not shown). More posterior regions of the stegostom were not reconstructed in this work. The protractors and marginal cells attach to three weak but distinct stylet knobs. The stylet protractor muscles are large, occupying most of the body cavity between where they originate and the level of the vestibule extension, anterior to which they attenuate to their insertion points on the cephalic framework (Figs. 3H and 4B). Anteriorly, the protractor muscles split into six branches (Fig. 5A), each corresponding to a blade of the framework. The splits between muscle branches are continued posteriad as distal grooves (Fig. 3H), in which the six pseudocoelomic cords of syncytial extensions and dendrites lie. Where the muscles attach to the stylet and the anterior pharyngeal lumen, they form the bulk of the feeding apparatus. The marginal cells are small in comparison and do not attach to the basal lamina of the pharynx, leaving large margins of contact between muscle cells. At the posterior end of the stylet knobs, the muscles show a strong diminution of contractile fibers, which disappear almost immediately in the pharynx. Posterior to the stylet the cytoplasm of the muscle cells persists as noncontractile and metabolic (not shown).

Pharyngeal Neuron

Also associated with the stylet apparatus is a pharyngeal neuron. This neuron runs through the pharynx, stegostom, and gymnostom between the right subdorsal marginal cell and the dorsal and right subventral protractor muscles, increasing in diameter anteriorly (Figs. 5B,D and 6), where in the gymnostom it swells to its largest in cross section and is full of microtubules and even includes mitochondria; anterior to this broad region it tapers and terminates abruptly. From its swollen tip the neuron sends a thin process (Fig. 6A) into the dorsal protractor muscle (Fig. 6B). The neuron maintains a close apposition with the right subdorsal marginal cell, the anterior tip of which is not far from the anterior tip of the neuron; where the neuron is most swollen, it makes an additional, limited apposition with the anterior tip of the left subdorsal marginal cell (Fig. 6B). The precise association of the neuron to muscle and marginal tissue is uncertain, although further study may elucidate the presence and extent of synapses.

DISCUSSION

With the example of the tylenchid stylet, we have demonstrated that apparent incongruence of morphological evolution and molecular phylogeny can be resolved upon closer examination of mor-

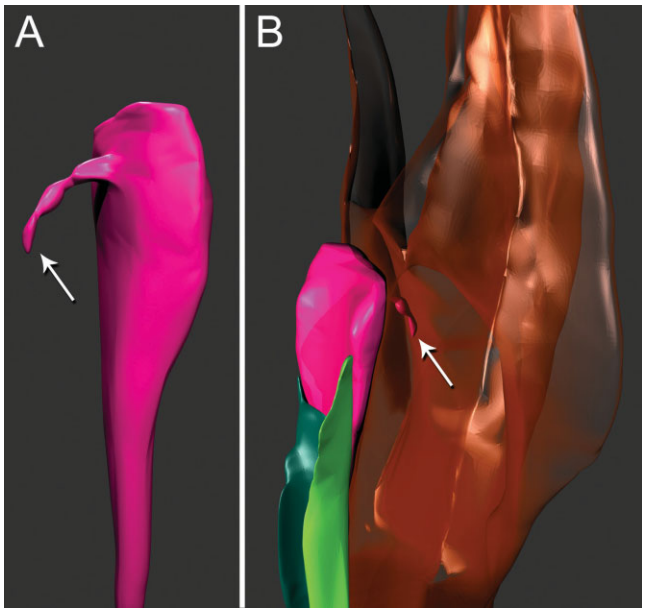

Fig. 6. Three-dimensional reconstructions of pharyngeal neuron and associated cells based on serial TEM sections of tissues of the stomatostylet apparatus of *Aphelenchus avenae*. Key to cells in Figure 2 applies where possible. **A:** Dorsolateral view of distal part of pharyngeal nerve dendrite (fuchsia). Arrow indicates fine pharyngeal nerve process. **B:** Ventrolateral view of pharyngeal nerve dendrite associated with left (green) and right (teal) subdorsal marginal cells and of fine nerve process (indicated by arrow) extending into dorsal stylet protractor muscle (brown, transparent).

phology. In spite of stark superficial differences in feeding structures between sister taxa, we have shown plausible morphological transformation of their component parts. This study used complete 3D reconstruction to recognize "minuteness of resemblance" to recover the functional hierarchy of putative homologs (Tyler, 1988), showing that stomatostylet characters are remarkably conserved at a cellular level.

Homologies of Anterior Tissues With Respect to Outgroups

Cheilostom. Epidermis reconstruction in *A. avenae* has allowed clear recognition of homologies with outgroups including a broad range of feeding types and associated stoma morphologies. Despite apparent differences due to divergent feeding structures, basic features of epidermal syncytium morphology are highly conserved with those in cephalobids and rhabditids (see Fig. 7). Comparisons with *A. complexus* are based on its reconstruction by Bumbarger et al. (2006), who also incorporated relevant unpublished data for *C. elegans* used by White et al. (1986). Proposed homologies in all three taxa of the cheilostom and other stylet regions are summarized in Table 2.

Putative HypE in *A. avenae* is similar in its basic morphology to HypE in *A. complexus*, forming a sheet-like toroid in the body wall, just anterior to the main mid body epidermal syncytium. Like HypE in *A. complexus* and homolog Hyp4 in *C. elegans*, it provides insertion points for anterior body wall muscles. This syncytium also serves to attach the stylet protractor muscles to the pharynx, in contrast to its homologs in either free-living outgroup. Although the lateral extensions were not traced to their absolute tips, they both attenuate posteriorly to a fine point in a manner similar to the lateral pseudosomal extensions of HypE in *A. complexus* and thus presumably also end without cell bodies containing nuclei.

The relationship of HypE in *A. avenae* to sensory structures is largely conserved. HypE is associated with the amphid and cephalic socket cells, as in both outgroup representatives. As in Hyp4 of *C. elegans*, HypE in *A. avenae* is also associated with the outer labial socket cells; however, *A. avenae* having this feature in common with *A. complexus* is precluded by the absence in *A. avenae* (and *C. elegans*) of the homolog of HypD, which is a minor syncytium forming an incomplete toroid positioned between the amphid and cephalic socket cells and

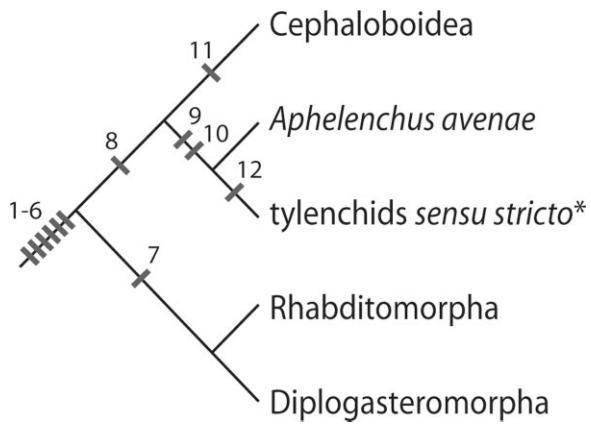

Fig. 7. Relationships of major groups based on published phylogenies inferred from 18S and 28S rRNA sequences (Aleshin et al., 1998; Blaxter et al., 1998; Holterman et al., 2006; Nadler et al., 2006; Smythe and Nadler, 2006; Meldal et al., 2007). Panagrolaimoidea and Aphelenchoidoidea, possibly comprising a monophyletic sister group to Cephaloboidea + *Aphelenchus* + tylenchids sensu stricto (Blaxter et al., 1998; Holterman et al., 2006; Meldal et al., 2007), are not shown due to their poor representation in stoma characters. Work is underway to address the morphological and molecular questions related to paraphyly of stomatostylet bearing organisms (Ragsdale, unpublished). Characters are mapped based on simple parsimony. 1–6, HypE, HypC, HypB, HypA, anterior arcade syncytium, and posterior arcade syncytium; 7, e1 and e3 (still requires outgroup representation to determine character polarity); 8, HypC containing multilamellar dendrite; 9, stomatostylet; 10, stomatal muscles inserting in cephalic framework; 11, HypD; 12, presence of secondary protractor muscle element (still requires outgroup representation to determine character polarity). *Non-aphelenchid Tylenchomorpha.

TABLE 2. Proposed homologies of stomatal and anterior epidermal tissues in Aphelenchus avenae (names given are putative), Acrobeles complexus, and Caenorhabditis elegans

A. avenae	*A. complexus*	*C. elegans*
HypE	HypE	Hyp4
Unknown	HypD	Unknown
HypC	HypC	Hyp3
HypB	HypB	Hyp2
HypA	HypA	Hyp1
Anterior arcade	Anterior arcade	Anterior arcade
Posterior arcade	Posterior arcade	Posterior arcade
Stylet protractors	ma	m1[a]
Unknown	mb	m2
Marginal cells	Marginal cells	Marginal cells (e2)
Unknown	Unknown	e1
Unknown	Unknown	e3

[a]Homologies of stomatal muscles in *A. complexus* and *C. elegans* proposed by Dolinski et al. (1998).

outer labial socket cells. The absence of HypD in all examined taxa other than *A. complexus* suggests that it is probably apomorphic for some clade of cephalobids. If regarded as such, comparisons present no problems of topological similarity, as the socket cells for all three types of sensilla are positioned between HypE and HypC in all three taxa.

Putative HypC of *A. avenae* is identical to that in *A. complexus* in having two dorsal somal extensions (two somal extensions and nuclei are also found in homolog Hyp3 of *C. elegans*). General morphology of the toroid is also similar between the two taxa in that it is marked by strong hexaradiate symmetry, which in *A. complexus* fills a shallow "framework" making up the base of the six cephalic probolae. An unidentified epidermal syncytium within a shallow framework was also noted in the cephalobid *Zeldia punctata* (Baldwin et al., 2004a). In *A. avenae*, however, HypC is greatly expanded anteriorly and medially with respect to cephalobids and rhabditids, and it is associated with a much deeper, more highly developed framework. The prominence of HypC in the head region has been accompanied by the shift of all other syncytia posterior to it along the central body axis; these syncytia have become concentrated into a relatively narrow column surrounding the vestibule extension and stylet.

Notwithstanding the absence of a homolog of HypD in *A. avenae*, association of HypC with the amphid, cephalic, and outer labial socket cells is conserved. Also conserved is the location of the inner labial sensilla, which are associated with the toroid of HypC posteriorly and medially. Unique to HypC in *A. avenae* are two pseudosomal extensions that each ensheathe a somatic nerve dendrite that terminates within the toroid. These two dendrites clearly branch into the elaborate multilamellar termini observed in the toroid of HypC (Fig. 4A,B), a phenomenon also observed in *A. complexus*, which led Bumbarger et al. (2006) to hypothesize the homolog of HypC in tylenchids based on existing TEM data of the tylenchid framework. Although these dendrites have been identified as homologs of dendrites (BAG) in *C. elegans* (Bumbarger et al., 2007), their expression in cephalobids and tylenchids seems to be unique and may, upon more extensive taxon sampling, be confirmed to constitute a synapomorphy for a clade of cephalobids and tylenchids.

Putative HypB of *A. avenae* is identical to HypB in *A. complexus* in having two somal extensions, one dorsal and one left subventral, the asymmetry of which also is shown in the two corresponding nuclei of homolog Hyp2 in *C. elegans*. Furthermore, the relationship of the anterior rim of the toroid with the inner labial socket cells is also conserved with outgroups. The morphology of the toroid is simple relative to *A. complexus*, there being no homologs in *A. avenae* of the pseudosomal extensions or anterior toroid processes observed in *A. complexus*. Although the points of contact with HypC give the appearance of processes, this is probably due to the toroid being constrained to the space between socket cells. The position of the inner labial socket cells and entry points of corresponding dendrites into the cuticle of the vestibule extension suggest that the anterior rim of the toroid has been oriented into a medial position in *A. avenae*, such that any potential homologs of the inner or outer toroid processes of HypC in *A. complexus* would be found in the position where the toroid meets the vestibule extension.

Putative HypA of *A. avenae* is identical to that in *A. complexus* in having three somal extensions, one dorsal and two subventral. As in *A. complexus*, the toroid of HypA is relatively simple in its morphology, being devoid of any processes other than somal extensions. Its toroid is the smallest of the anterior epidermal syncytia, as it is also in *A. complexus* (with the possible exception of HypD) and *C. elegans*.

Gymnostom. Two arcade syncytia were identified in *A. avenae*, confirmed by the numbers and positions of their somal extensions being conserved with respect to *A. complexus*, and to the number of nuclei in the arcade cells of *C. elegans* (Wright and Thomson, 1981). In other respects, arcade syncytium morphology is quite divergent relative to *A. complexus*. In contrast to the highly complex toroids of the latter, the arcade cell toroids of *A. avenae* lack any processes or extensions other than the somal extensions. It has been observed that in *A. complexus* the somal extensions of other anterior syncytia seem to cluster around those of the posterior arcade syncytium, which are relatively large in cross section. In *A. avenae* the posterior arcade somal extensions are likewise distributed among six pseudocoelomic cords. Although the reduction in diameter of these extensions in *A.*

avenae precludes such clustering, the posterior arcade syncytium nevertheless makes several contacts with other anterior syncytia through its somal extensions. The arcade toroids themselves are also diminutive with respect to *A. complexus*. The arcade syncytia of tylenchids seem to be highly active in development during production of the stylet shaft and cone, when their cytoplasm is full of mitochondria and secretory granules (Endo, 1985). By contrast, the apparent reduction in size and relative lack of organelles in the cytoplasm of the arcade syncytia in the adults suggest possible degeneration of function apart from a simply physical one of being a loose "membranous fold" or guide ring that allows protrusion of the stylet while keeping it attached to the vestibule extension (Baldwin and Hirschmann, 1976).

Stegostom. Reconstruction of stylet protractor muscle cells has provided more detailed evidence of their topological similarity, at their points of attachment to the stylet knobs, to the anteriormost three radial stomatal muscles of microbivores. However, in *A. avenae* these pharyngeal muscles are unique in having insertions in syncytium HypE. Although pharyngeal musculature does not terminate in the epidermis in *A. complexus* or *C. elegans*, tendon organs connecting the basal lamina of the anterior pharynx to the anterior termini of body wall muscles have been observed in both outgroups, *A. complexus* and *C. elegans*, which Bumbarger et al. (2006) postulated may have played a role in the evolution of stylet protractor muscles from simple, radial stomatal muscles. Reconstruction of these cells in earlier developmental stages may reveal the presence of such structures, which when combined with a more detailed knowledge of their distribution in a cephalobid outgroup, may provide additional support for the homology of the stylet protractors with the m1 cells of the prostegostom. The triradiate marginal cells that lie between stylet protractors, and more posteriorly, other pharyngeal cells are presumably the homologs of those found in free-living outgroups (i.e., "e2" of *C. elegans*), a notable difference being their nonattachment to the pharyngeal basal lamina in *A. avenae*.

Precise identities of other stomatal muscles are still unknown. Preliminary results of serial sectioning through the pharynx reveal an absence of contractile muscle cells in the procorpus posterior to the stylet protractors. The plasticity of stegostom and pharynx elements between cephalobids and tylenchids is not yet known, although at least some characters are divergent between cephalobids and rhabditids (Dolinski et al., 1998). Whether the homologs of m2 cells or secondary protractor muscles are present in *A. avenae*, but expressed differently, remains to be determined by reconstruction of the pharynx, which would provide necessary tests of conjunction.

Epithelial toroids e1 and e3, which make up the anterior stegostom of rhabditids and diplogastrids (Baldwin et al., 1997a,b), are not found in *A. avenae*. This absence would be predicted from their absence in cephalobids (Dolinski et al., 1998) and common ancestry of rhabditids and diplogastrids exclusive of cephalobids and tylenchids (see Fig. 7).

Homologies of Anterior Tissues With Respect to Other Tylenchomorpha

The complexity of anterior epidermal cells in other tylenchids has precluded their precise characterization heretofore. Reviewing existing micrographs of the head region of tylenchids, Baldwin et al. (2004a) identified at least four syncytial toroids surrounding the stylet and guiding apparatus, although the most anterior epidermis remained elusive. Reexamination of published tylenchid fine structure research shows what appear to be the multilamellar dendrites within HypC to be present in the unidentified head epidermis of various other tylenchids, for example, *Meloidogyne incognita* (Baldwin and Hirschmann, 1976), *Heterodera glycines* (Baldwin and Hirschmann, 1976; Endo, 1983, 1985), and *Pratylenchus penetrans* (Endo et al., 1997). The conservation of this feature with outgroups suggests that HypC is present and characterized by an association with this dendrite in other Tylenchomorpha. Arcade syncytia have been previously observed in molting *H. glycines* in the region of the stylet (Endo, 1985). Four syncytia were considered "arcade-like cells," although the anterior two were most likely the HypA and HypB syncytia, which were in a comparable position to those toroids in *A. avenae*. The primary stylet protractors of *A. avenae* are very similar in morphology and positional topology to the primary protractors in other Tylenchomorpha. The branching of the primary protractors is identical with those in *M. incognita* and *H. glycines* (Baldwin and Hirschmann, 1976) as well as in the aphelenchoid nematode *Aphelenchoides blastophthorus* (Shepherd et al., 1980). Insertions of muscles through the epidermis into the posterior margins of the blades of the framework in *A. avenae* are consistent with the situation in *H. glycines* juveniles (Endo, 1983) and *Hexatylus viviparus* (Shepherd and Clark, 1976), and apparently also with *A. blastophthorus* (Shepherd et al., 1980), although limited detail in the latter precludes adequate comparison. Notably missing in *A. avenae* are "secondary muscle elements," which are thin strips of protractor muscle apparently attaching to the pharyngeal lumen just posterior to the stylet knobs, observed in *M. incognita* and *H. glycines*. These were originally hypothesized to be the homologs of the m2 muscles of the cephalobid mesostegostom (Baldwin et al., 2004a). Interestingly, secondary protractor muscles are found in *A. blastophthorus*, where they are

much more pronounced than they are in *M. incognita* and *H. glycines*. The relative locations and branching patterns of these cells seem to be identical in those taxa possessing them, the subventral secondary protractors being unbranched and associated with the distal borders of the subventral primary protractors, and the dorsal protractors splitting into two branches that are both associated with the dorsal primary protractor.

Homologies of the Stomatostylet and Other Cuticular Structures

Confirming the identities of epidermal tissues allows for more reasonable hypotheses of homology concerning the cuticular structures that they produce, which in their differences in feeding function are morphologically divergent between tylenchids and cephalobids. HypE in *A. avenae* underlies the cuticle of the cephalic body wall just posterior to the cephalic framework, a feature that is conserved with *A. complexus* and *C. elegans*, in both of which HypE is posterior to what is considered labial cuticle. HypC is associated with outer (distal) labial cuticle in outgroups, including the cephalic probolae in *A. complexus*. HypB is associated with inner (medial) labial cuticle in outgroups, which in *A. complexus* includes the labial probolae. HypA, as in outgroups, is associated with a ring of the most inner labial cuticle, which is at the interface with the cuticle immediately surrounding the mouth opening.

In *A. avenae* the two arcade syncytium toroids are associated with the stylet shaft; in cephalobids and rhabditids they line the gymnostom. Interestingly, in many other Chromadorea, including cephalobids, this cuticle comprises a cylindrical, anterior projection separating the buccal capsule from the rest of the labial cuticle around it, a feature in common noted by Baldwin et al. (2004a) in formulating their revised hypothesis of gymnostom homology. These results are consistent with ultrastructure of the molt of *H. glycines* (Endo, 1985) where it was observed that four "arcade like cells" supported the stylet cone and shaft as well as the "stomatal wall" (cheilostom); the posterior (two) of these were presumably responsible for the stylet shaft cuticle. It is known that the arcade cells secrete the gymnostom in *C. elegans* (Wright and Thomson, 1981).

As in other tylenchids, the stylet shaft and cone of *A. avenae* are distinct in the types of cuticle making up the bulk of their structure. Yet differences in cuticular patterns seem to be evident in various taxa, including "alternating bands" of cuticle in the stylet of *H. viviparus* (Shepherd and Clark, 1976) and longitudinal ducts in the stylet shaft of *Mesocriconema xenoplax* (Chen and Wen, 1980). The stylet cuticle of *A. blastophthorus*, also composed of at least two major, distinct components defining these regions, was described as being very complex, a notable difference being the presence of "channels" within the cuticle of the stylet shaft (Shepherd et al., 1980). Although true differences between the stylet of *A. blastophthorus* and those of *A. avenae* and tylenchids sensu stricto (i.e., non-aphelenchid Tylenchomorpha) would prove phylogenetically significant, current comparison is limited by compatibility of data. It is difficult to tell which differences in poorly characterized tissue elements are due to fixation and/or staining between researchers or fundamental differences in cuticular ultrastructure.

In *A. avenae*, as in other studied Tylenchomorpha, the cuticle of the stylet knobs seems to be continuous with that of the stylet shaft. In all cases, however, different tissues line these separate areas and suggest at least partially separate origins of these structures. Endo (1985) showed that the stylet knobs formed in vacuoles separate from the shaft and cone in the pharynx, presumably secreted by the marginal cells.

Implications for the Evolution of Plant Parasitism

Differences between stomatostylet bearing nematodes and microbivores. Comparative, detailed morphology of feeding structures has now provided a basis for future studies on the evolution of parasitism, for which the stylet appears to be a requirement (Baldwin et al., 2004b). Knowledge of the structures of cells and the connections between them, and how these are variously distributed across a phylogeny, establishes a model for testing functional biology. Some fields for further investigation include looking at the most striking differences between homologs in *A. avenae* and *A. complexus*, for example: in the musculature, which is characterized by different anterior insertion points in taxa with different feeding behaviors; of the arcade cells, whose complexity in *A. complexus* is exaggerated immensely with respect to the diminutive guide ring in *A. avenae*; and of the prominence of HypC in the head region in *A. avenae*. Differences in morphology could be explored further, such as the possible extension of muscles into the framework epidermis by way of tendon organs during ontogeny.

Diversity of the stylet within tylenchids. On a gross level the stomatostylet is characterized by a diversity of sizes, relative sizes of components, and component shapes, accompanied by a wide range of feeding behaviors (Dropkin, 1969). *Aphelenchus avenae* is a fungivore, as are probably many other taxa basal (i.e., branching near the root) within the Tylenchomorpha (Yeates et al., 1993). Such basal taxa are often characterized by a "weak" stylet, as has been demonstrated herein for *A. avenae*. *Aphelenchus avenae* is presently

regarded to be the sister group of all other tylenchids sensu stricto; consequently, the relatively wide stylet lumen and large stylet orifice, compared with those of all other tylenchids examined, may fit expectations for a transitional state between the open stoma of microbivores and those tylenchids feeding strictly on host cytoplasm. Exploring differences in homologies on a fine structural level between *A. avenae* and more apical tylenchids would offer insight into the evolution of parasitism, given the preexisting adaptation of the stomatostylet apparatus.

Independent evolution of the stomatostylet?. Phylogenies that have been inferred from rRNA sequences suggest paraphyly of the Tylenchomorpha. The Aphelenchoidoidea appear as a lineage independent of Aphelenchidae plus tylenchids sensu stricto; the two clades are apparently nested within different superfamilies of cephalobids, the Panagrolaimoidea and Cephaloboidea, respectively (Blaxter et al., 1998; Holterman et al., 2006; Meldal et al., 2007). The implications of extant phylogeny for independent evolution of the stomatostylet are striking. Although Siddiqi (1980) hypothesized independent origins of "Aphelenchida" (a taxon of traditional classifications grouping Aphelenchoidoidea and Aphelenchidae) and tylenchids sensu stricto, most traditional systems recognize a general affinity of these two groups (Paramonov, 1960; Andrássy, 1976; Maggenti, 1981;). In recent studies, incongruence with classical hypotheses has been suggested to be a consequence of artifact in analysis (Holterman et al., 2006).

Musculature comprises the best documented and most readily comparable element of the stomatostylet apparatus across stomatostylet bearing nematodes. Patterns of splitting in primary protractor muscles are the same in all taxa examined. Whether this is the result of convergence because of the functional constraints in the way triradiate muscles can attach to a hexaradiate framework, the result of shared ancestry of all stomatostylet bearing nematodes, or both (such as by parallel evolution) remains a question dependent upon greater resolution of the relationships between these taxa and outgroups. The presence of a similar pharyngeal neuron associated with the stylet musculature is an interesting shared character common to both *Aphelenchus avenae* and *Aphelenchoides blastophthorus*. Inspection of unpublished TEM micrographs indicates that the homolog of this neuron may be present in other tylenchids such *as M. incognita* and *H. glycines*, although if so it is not expressed so prominently. Precise identification and greater taxon sampling should reveal the phylogenetic significance of this character across stomatostylet bearing nematodes. Furthermore, the possible homolog of this neuron in *A. complexus* is not known. Discovery of this character in the context of precise pharyngeal nerve maps of *C. elegans* (Albertson and Thomson, 1976; White et al., 1986), if shown to be conserved to the level of other feeding related structures, could provide another test of congruence of stegostom homologies.

Homologies of anterior syncytia in nematodes with stomatostylets are not yet characterized to the degree of those of *A. avenae*, and are thus not as easily comparable. Yet the model established for *A. avenae* can be readily extended to other taxa, given the compelling amount of conservation of these structures between widely varying mouthpart morphologies. Of particular interest is the position of the dorsal gland orifice (DGO), which is located closely posterior to the base of the stylet in tylenchids sensu stricto but relatively far posteriad in the large metacorpi of *A. avenae* (Aphelenchidae) and Aphelenchoidoidea. The position of the DGO has been an important taxonomic character in dividing tylenchids from "Aphelenchida." Furthermore, the position varies considerably within tylenchids sensu stricto. Reconstruction of this character including the associated pharynx in representatives of all three taxa may supply morphological evidence for resolving their interrelationships. Additional evidence will be required for stronger tests of congruence, including sequences from alternate loci to complement rRNA datasets, especially from currently undersampled groups. Other independent morphological evidence, such as characters of conserved sensory structures, is also significant given the current paucity of congruent characters for more inclusive clades, particularly a clade exclusive to cephalobids and tylenchids.

ACKNOWLEDGMENTS

The authors thank Sitara Wijeratne and Cale Carter for their valuable contributions in manual section alignment and cell tracing, and Dan Bumbarger for his comments and generous technical assistance.

LITERATURE CITED

Albertson DG, Thomson JN. 1976. The pharynx of *Caenorhabditis elegans*. Philos Trans Royal Soc Lond B 275:299–325.

Aleshin VV, Kedrova OS, Milyutina IA, Vladychenskaya NS, Petrov NB. 1998. Relationships among nematodes based on the anlysis of 18S rRNA gene sequences: Molecular evidence for monophyly of chromadorian and secernentean nematodes. Russ J Nematol 6:175–184.

Andrássy I. 1962. Über den mundstachel der tylenchiden (Nematologische Notizen, 9). Acta Zool Hung 8:167–315.

Andrássy I. 1976. Evolution as a Basis for the Systemization of Nematodes. London: Pitman Publishing.

Baldwin JG, Eddleman CD. 1995. Buccal capsule of *Zeldia punctata* (Nemata: Cephalobidae): An ultrastructural study. Can J Zool 73:648–656.

Baldwin JG, Hirschmann H. 1976. Comparative fine structure of the stomatal region of males of *Meloidogyne incognita* and *Heterodera glycines*. J Nematol 8:1–17.

Baldwin JG, Giblin-Davis RM, Eddleman CD, Williams DS, Vida JT, Thomas WK. 1997a. The buccal capsule of *Aduncospiculum halicti* (Nemata: Diplogasterina): An ultrastructural and molecular phylogenetic study. Can J Zool 75:407–423.

Baldwin JG, Frisse LM, Vida JT, Eddleman CD, Thomas WK. 1997b. An evolutionary framework for the study of developmental evolution in a set of nematodes related to *Caenorhabditis elegans*. Mol Phylogenet Evol 8:249–259.

Baldwin JG, Bumbarger D, Ragsdale E. 2004a. Revised hypotheses for phylogenetic homology of the stomatostylet in tylenchid nematodes. Nematology 6:623–632.

Baldwin JG, Nadler SA, Adams BJ. 2004b. Evolution of plant parasitism among nematodes. Ann Rev Phytopathol 16:83–105.

Blaxter M, De Ley P, Garey JR, Liu LX, Scheldeman P, Vierstraete A, Vanfleteren JR, Mackey LY, Dorris M, Frisse LM, Vida JT, Thomas WK. 1998. A molecular evolutionary framework for the phylum Nematoda. Nature 392:71–75.

Bumbarger DJ, Crum J, Ellisman MH, Baldwin JG. 2006. Three-dimensional reconstruction of the nose epidermal cells in the microbial feeding nematode. *Acrobeles complexus* (Nematoda: Rhabditida). J Morphol 267:1257–1272.

Bumbarger DJ, Crum J, Ellisman MH, Baldwin JG. 2007. Three-dimensional fine structural reconstruction of the nose sensory structures of Acrobeles complexus compared to *Caenorhabditis elegans* (Nematoda: Rhabditida). J Morphol 268: 649–663.

Chen TA, Wen G-Y. 1980. Electron microscopy of the stomatostylet and esophagus of *Criconemoides curvatum*. J Nematol 12:72–83.

De Grisse AT. 1972. Elektromikroskopische waarnemingen aangaande de structuur van de stekelschede in Tylenchiden. Med Fak Landbouww Rijksuniv Gent 37:323–327.

De Ley P, Blaxter M. 2002. Systematic position and phylogeny. In: Lee DL, editor. The Biology of Nematodes. London: Taylor & Francis. pp 1–30.

De Ley P, Blaxter ML. 2004. A new system for Nematoda: combining morphological characters with molecular trees, and translating clades into ranks and taxa. In: Cook R, Hunt DJ, editors. Proceedings of the Fourth International Congress of Nematology, June 8–13, 2002, Tenerife, Spain. Leiden: Brill. pp 633–653.

De Ley P, Van de Velde MC, Mounport D, Baujard P, Coomans. 1995. Ultrastructure of the stoma in Cephalobidae, Panagrolaimidae, and Rhabditidae, with a proposal for a revised ptoma terminology in Rhabditida (Nematoda). Nematologica 41:153–182.

Dolinski C, Borgonie G, Schnabel R, Baldwin JG. 1998. Buccal capsule development as a consideration for phylogenetic analysis of Rhabditida (Nemata). Dev Genes Evol 208:495–503.

Dropkin VH. 1969. Cellular responses of plants to nematode infections. Ann Rev Phyopathol 7:101–122.

Endo BY. 1983. Ultrastructure of the stomatal region of the juvenile stage of the soybean cyst nematode. Heterodera glycines. Proc Helminthol Soc Wash 50:43–61.

Endo BY. 1985. Ultrastructure of the head region of molting second-stage juveniles of Heterodera glycines with emphasis on stylet formation. J Nematol 17:112–123.

Endo BY, Zunke U, Wergin WP. 1997. Ultrastructure of the lesion nematode. *Pratylenchus penetrans* (Nemata: Pratylenchidae). J Helminthol Soc Wash 64:59–95.

Goodey JB. 1963. Speculations on the identity of the parts of the tylenchid spear. Nematologica 9:468–470.

Holterman M, van der Wurff A, van den Elsen S, van Megen H, Bongers T, Holovachov O, Bakker J, Helder J. 2006. Phylum-wide analysis of SSU rDNA reveals deep phylogenetic relationships among nematodes and accelerated evolution toward crown clades. Mol Biol Evol 23:1792–1800.

Hunt DJ. 1993. Aphelenchida, Longidoridae, and Trichodoridae: Their Systematics and Bionomics. Wallingford, UK: CAB International.

Kremer JR, Mastronarde DN, McIntosh JR. 1996. Computer visualization of three-dimensional image data using IMOD. J Struct Biol 116:71–76.

Maggenti A. 1981. General Nematology. New York: Springer-Verlag.

Meldal BH, Debenham NJ, De Ley P, De Ley IT, Vanfleteren JR, Vierstraete AR, Bert W, Borgonie G, Moens T, Tyler PA, Austen MC, Blaxter ML, Rogers AD, Lambshead PJ. 2007. An improved molecular phylogeny of the Nematoda with special emphasis on marine taxa. Mol Phylogenet Evol 42:622–636.

Nadler SA, De Ley P, Mundo-Ocampo M, Smythe AB, Stock SP, Bumbarger D, Adams BJ, De Ley IT, Holovachov O, Baldwin, JG. 2006. Phylogeny of Cephalobina (Nematoda): Molecular evidence for recurrent evolution of probolae and incongruence with traditional classifications. Mol Phylogentet Evol 40:696–711.

Panchen AL. 1994. Richard Owen and the concept of homology. In: Hall BK, editor. Homology: The Hierarchical Basis of Comparative Biology. London: Academic Press. pp 21–62.

Paramonov AA. 1960. Skrjabin, K, editor. Plant-Parasitic Nematodes, Vol. 1. Jerusalem: Israel Program for Scientific Translations.

Patterson C. 1982. Morphological characters and homology. In: Joysey KA, Friday AE, editors. Problems of Phylogenetic Peconstruction. London: Academic Press. pp 21–74.

Shepherd AM, Clark SA. 1976. Structure of the anterior alimentary tract of the passively feeding nematode *Hexatylus viviparus* (Neotylenchidae: Tylenchida). Nematologica 22: 332–342.

Shepherd AM, Clark SA, Hooper DJ. 1980. Structure of the anterior alimentary tract of *Aphelenchoides blastophthorus* (Nematoda: Tylenchida. Aphelenchina). Nematologica 26:313–357.

Siddiqi MR. 1980. The origin and phylogeny of the nematode orders Tylenchida Thorne, 1949 and Aphelenchida n. ord. Helminthol Abstr B Plant Nematol 49:143–170.

Siddiqi MR. 2002. Tylenchida: Parasites of Plants and Insects. Wallingford, UK: CAB International.

Smythe AB, Nadler SA. 2006. Nematode small subunit phylogeny correlates with alignment parameters. Syst Biol 55:972–992.

Steiner G. 1933. The nematode *Cylindrogaster longistoma* (Stefanski) Goodey, and its relationship. J Parasitol 20:66–69.

Thorne G. 1961. Principles of Nematology. New York: McGraw-Hill.

Tyler S. 1988. The role of function in determination of homology and convergence—examples from invertebrate adhesive organs. Prog Zool 36:331–347.

Van de Velde MC, De Ley P, Mounport D, Baujard P, Coomans A. 1994. Ultrastructure of the buccal cavity and the cuticle of three Cephalobidae (Nematoda: Rhabditida). Nematologica 40:541–563.

White JG, Southgate E, Thomson JN, Brenner S. 1986. The structure of the nervous system of *Caenorhabditis elegans*. Philos Trans Royal Soc Lond B 341:1–340.

Wright KA, Thomson JN. 1981. The buccal capsule of *Caenorhabditis elegans* (Nematoda: Rhabditoidea): An ultrastructural study. Can J Zool 59:1952–1961.

Yeates GW, Bongers T, de Goede RGM, Freckman DW, Georgieva SS. 1993. Feeding-habits in soil nematode families and genera—an outline for soil ecologists. J Nematol 25:315–331.